isvr Institute of Sound and Vibration Research

Finite Element Addendum for BEASTS

I. Anderson and C.J.C. Jones

ISVR Technical Memorandum No 881

February 2002

University of Southampton

SCIENTIFIC PUBLICATIONS BY THE ISVR

Technical Reports are published to promote timely dissemination of research results by ISVR personnel. This medium permits more detailed presentation than is usually acceptable for scientific journals. Responsibility for both the content and any opinions expressed rests entirely with the author(s).

Technical Memoranda are produced to enable the early or preliminary release of information by ISVR personnel where such release is deemed to the appropriate. Information contained in these memoranda may be incomplete, or form part of a continuing programme; this should be borne in mind when using or quoting from these documents.

Contract Reports are produced to record the results of scientific work carried out for sponsors, under contract. The ISVR treats these reports as confidential to sponsors and does not make them available for general circulation. Individual sponsors may, however, authorize subsequent release of the material.

UNIVERSITY OF SOUTHAMPTON
INSTITUTE OF SOUND AND VIBRATION RESEARCH
DYNAMICS GROUP

Finite Element Addendum for BEASTS

By

L. Andersen and C.J.C. Jones

ISVR Technical Memorandum No: 881

February 2002

Authorised for issue by
Dr. M.J. Brennan
Group Chairman

Summary

This report is an addendum to the previously published Technical Memoranda 867 and 868 [3, 2], where the computer program BEASTS, which may be used for elastodynamic boundary element analysis of three-dimensional continua, was presented. In this report a number of finite elements are presented which have been implemented in the computer program, so that a coupled finite element-boundary element analysis may be performed for structure-soil interaction problems such as railway tunnels exposed to harmonic excitation. The theory for the finite element part of the model is explained and an extension to the user manual for BEASTS [2] is presented. Finally, a numerical example is given, in which a rectangular foundation on a layered half-space is analysed.

Contents

1 Introduction 1

2 The Formulation of a Finite Element Domain 1

3 Three-dimensional Continuum Finite Elements 4
3.1 Hexahedron with 8 Nodes (Element Type 1) 5
3.2 Hexahedron with 18 Nodes (Element Type 2) 6
3.3 Hexahedron with 26 Nodes (Element Type 3) 7
3.4 Hexahedron with 21 Nodes (Element Type 4) 8
3.5 Hexahedron with 13 Nodes (Element Type 5) 9
3.6 Hexahedron with 17 Nodes (Element Type 6) 10
3.7 Hexahedron with 20 Nodes (Element Type 7) 11
3.8 Hexahedron with 23 Nodes (Element Type 8) 12
3.9 Triangular Prism with 12 Nodes (Element Type 9) 13
3.10 Triangular Prism with 18 Nodes (Element Type 10) 14
3.11 Triangular Prism with 15 Nodes (Element Type 11) 15

4 Data Preparation 16
4.1 General Data Specification 16
4.2 The **Finite Elements* Module 16
4.3 The **Boundary Element Domain* Module, revisited 18
4.4 Setting the Number of Nodes Allowed in the Input Data 18

5 Numerical Examples 19
5.1 Case 1: Vertically Excited Foundation on a Layered Half-Space 19
5.2 Case 2: Horizontally Excited Foundation on a Layered Half-Space 22

6 Conclusions 24

Acknowledgement 24

References 24

A BEASTS input: Model 1 25

B BEASTS input: Model 2 27

1 Introduction

Boundary elements (BE) are efficient for the analysis of unbounded media and the results obtained with the boundary element method (BEM) are very precise. However, the BEM is not suitable for analysis of structures where the material parameters are rapidly changing with the distance or where fine geometries must be modelled. In that case a finite element method (FEM) solution is appropriate. Finite elements (FE) are therefore preferred for the analysis of, for example, thin structures and media with local inhomogeneities.

In Reference [3] a boundary element scheme for three-dimensional elastodynamic analysis of bounded or unbounded domains was developed. The user documentation for the computer program BEASTS (Boundary Element Analysis of Soil and Three-dimensional Structures) based on the theory explained in Reference [3] was given in Reference [2]. In the original version of BEASTS, no finite elements were available. For the purpose of analysing such structures as bored tunnels with a concrete lining or a surface railway on a slab track, finite elements are now implemented. The implementation is straight forward as the coupling of multiple boundary element sub-domains in a single model is already performed in terms of nodal forces, that is by a transformation of the BE system matrices into an equivalent FE stiffness matrix.

Continuum finite elements are found to be suitable for modelling such structures as tunnel walls or railway tracks. They may be coupled to the existing boundary element types in BEASTS so that the conforming condition is satisfied. This does not apply to structural elements, such as shell elements. The latter may lead to more extra degrees of freedom than are needed when continuum finite elements are used. Finally, for continuum finite elements, a simple way of including wave-transmitting boundaries exists by means of coupling with an open boundary element domain.

In the following sections the theory for a finite element domain is described briefly, and the various finite element types available in the revised version of BEASTS are presented. The shape functions for each finite element type are listed, and the input data definition that is used in BEASTS is explained.

2 The Formulation of a Finite Element Domain

Consider an elastic body Ω which has the surface Γ with the outward unit normal vector $\mathbf{n}$. In Cartesian coordinates, x_j, the time domain equation of motion becomes,

$$\frac{\partial}{\partial x_j}\sigma_{ij}(\mathbf{x},t) + \rho(\mathbf{x})\, b_i(\mathbf{x},t) = \rho(\mathbf{x})\, \frac{\partial^2}{\partial t^2} u_i(\mathbf{x},t)\,, \tag{1}$$

where $\sigma_{ij}(\mathbf{x},t)$ is the *Cauchy stress tensor*, $u_i(\mathbf{x},t)$ is the displacement field, $\rho(\mathbf{x})$ is the mass density and $b_i(\mathbf{x},t)$ is the load per unit mass. Vector $\mathbf{x}$ is the position in space and t is the time. The summation convention applies, *i.e.* summation is performed over repeated indices.

Assuming small (linear) deformations, the relationship between the stress field and the strain field is given by *Hooke's generalized law*,

$$\sigma_{ij}(\mathbf{x},t) = D_{ijkl}(\mathbf{x})\, \epsilon_{kl}(\mathbf{x},t)\,, \quad \epsilon_{ij}(\mathbf{x},t) = \frac{1}{2}\left(\frac{\partial}{\partial x_i} u_j(\mathbf{x},t) + \frac{\partial}{\partial x_j} u_i(\mathbf{x},t)\right), \tag{2}$$

where $\epsilon_{ij}(\mathbf{x},t)$ is the *infinitesimal strain tensor* and $D_{ijkl}(\mathbf{x})$ is referred to as the *elasticity tensor*.

The finite element formulation is based on the weak form of the field equations which is obtained by multiplication of Equation (1) with the arbitrary weight function $\tilde{u}_i(\mathbf{x},t)$ and integration over the volume. Making use of the Green's theorem, the following integral equation is obtained for the domain Ω,

$$\int_\Omega \tilde{\epsilon}_{ij}(\mathbf{x},t)\,\sigma_{ij}(\mathbf{x},t)\,dV + \int_\Omega \tilde{u}_i(\mathbf{x},t)\,\rho(\mathbf{x})\,\frac{\partial^2}{\partial t^2}u_i(\mathbf{x},t)\,dV = \int_\Gamma \tilde{u}_i(\mathbf{x},t)\,p_i(\mathbf{x},t)\,dS + \int_\Omega \tilde{u}_i(\mathbf{x},t)\,\rho(\mathbf{x})\,b_i(\mathbf{x},t)\,dV. \quad (3)$$

$\tilde{\epsilon}_{ij}(\mathbf{x},t)$ is the strain related to the virtual field $\tilde{u}_i(\mathbf{x},t)$ and $p_i(\mathbf{x},t) = \sigma_{ij}(\mathbf{x},t)\,n_j(\mathbf{x})$ is the surface traction. Here n_j are the components of the outward unit normal vector. Use has been made of the fact that $\sigma_{ij}(\mathbf{x},t) = \sigma_{ji}(\mathbf{x},t)$ so that $(\partial\tilde{u}_i(\mathbf{x},t)/\partial x_j)\;\sigma_{ij}(\mathbf{x},t) = (\partial\tilde{u}_j(\mathbf{x},t)/\partial x_i)\;\sigma_{ij}(\mathbf{x},t)$. Equation (3) may alternatively be derived by applying *Hamilton's principle*, see Reference [1].

The next step in the FE approach is to discretize the domain into a number of finite elements. The displacement field and the virtual field are only evaluated at a finite number of nodes and approximated over the rest of the domain using shape functions. In the finite element method the shape functions are defined locally in each element as opposed to the Rayleigh-Ritz method where the shape functions are global. Let $\mathbf{u}_j(t)$ and $\tilde{\mathbf{u}}_j(t)$ be two $(3N_j \times 1)$ vectors storing the nodal displacements in the physical and the virtual field, respectively, for the N_j nodes in element j. Furthermore defining $\mathbf{x}_j$ as the $(3N_j \times 1)$ coordinate vector for the element nodes, the displacement field, the virtual field over the element volume Ω_j and the geometry may each be described in vector form,

$$\mathbf{u}(\mathbf{x},t) = \mathbf{\Phi}_j(\mathbf{x})\,\mathbf{u}_j(t)\,, \quad \tilde{\mathbf{u}}(\mathbf{x},t) = \mathbf{\Phi}_j(\mathbf{x})\,\tilde{\mathbf{u}}_j(t)\,, \quad \mathbf{x} = \mathbf{\Phi}_j(\mathbf{x})\,\mathbf{x}_j, \quad (4)$$

where $\mathbf{x}$ is a point (x_1, x_2, x_3) in the interior Ω_j of the element and $\mathbf{\Phi}_j(\mathbf{x})$ is a $(3 \times 3N_j)$ matrix storing the shape functions for the element,

$$\mathbf{\Phi}_j(\mathbf{x}) = \begin{bmatrix} \phi_1 & 0 & 0 & \phi_2 & 0 & 0 & \cdots & \phi_{N_j} & 0 & 0 \\ 0 & \phi_1 & 0 & 0 & \phi_2 & 0 & \cdots & 0 & \phi_{N_j} & 0 \\ 0 & 0 & \phi_1 & 0 & 0 & \phi_2 & \cdots & 0 & 0 & \phi_{N_j} \end{bmatrix}. \quad (5)$$

Each of the components ϕ_n, $n = 1, 2, \ldots, N_j$, is the shape function belonging to the nth element node and depends on the position $\mathbf{x}$ inside the element. The Galerkin method is used, *i.e.* the shape functions for the physical field and the virtual field are identical. Note that in the BEM the Green's functions are used as weight functions so that the virtual field is defined globally.

Next, assume that the medium is locally homogeneous and isotropic over each element. The material is defined by the mass density ρ_j, the Young's modulus E_j and the Poisson ratio ν_j. For the individual finite element the discretized equation of motion may then conveniently be written in the form

$$\{\tilde{\mathbf{u}}_j(t)\}^T \left(\int_{\Omega_j} \{\tilde{\mathbf{\nabla}}\mathbf{\Phi}_j(\mathbf{x})\}^T \mathbf{D}_j \tilde{\mathbf{\nabla}}\mathbf{\Phi}_j(\mathbf{x})\,dV\;\mathbf{u}_j(t) + \int_{\Omega_j} \{\mathbf{\Phi}_j(\mathbf{x})\}^T \rho_j \mathbf{\Phi}_j(\mathbf{x})\,dV\;\frac{\partial^2}{\partial t^2}\mathbf{u}_j(t) \right) = \{\tilde{\mathbf{u}}_j(t)\}^T \left(\int_{\Gamma_j} \{\mathbf{\Phi}_j(\mathbf{x})\}^T \mathbf{p}(\mathbf{x},t)\,dS + \int_{\Omega_j} \{\mathbf{\Phi}_j(\mathbf{x})\}^T \rho_j \mathbf{b}(\mathbf{x},t)\,dV \right), \quad (6)$$

where $\mathbf{p}(\mathbf{x},t)$ and $\mathbf{b}(\mathbf{x},t)$ are the surface traction and the body force with the components $p_i(\mathbf{x},t)$ and $b_i(\mathbf{x},t)$, $i = 1,2,3$, respectively. $\tilde{\boldsymbol{\nabla}}$ is a matrix differential operator defined as

$$\tilde{\boldsymbol{\nabla}} = \begin{bmatrix} \frac{\partial}{\partial x_1} & 0 & 0 & \frac{\partial}{\partial x_2} & \frac{\partial}{\partial x_3} & 0 \\ 0 & \frac{\partial}{\partial x_2} & 0 & \frac{\partial}{\partial x_1} & 0 & \frac{\partial}{\partial x_3} \\ 0 & 0 & \frac{\partial}{\partial x_3} & 0 & \frac{\partial}{\partial x_1} & \frac{\partial}{\partial x_2} \end{bmatrix}^T , \tag{7}$$

and $\mathbf{D}_j$ is the elasticity tensor rearranged in matrix form,

$$\mathbf{D}_j = \frac{E_j}{(1+\nu_j)(1-2\nu_j)} \begin{bmatrix} 1-\nu_j & \nu_j & \nu_j & 0 & 0 & 0 \\ \nu_j & 1-\nu_j & \nu_j & 0 & 0 & 0 \\ \nu_j & \nu_j & 1-\nu_j & 0 & 0 & 0 \\ 0 & 0 & 0 & \frac{1}{2}(1-2\nu_j) & 0 & 0 \\ 0 & 0 & 0 & 0 & \frac{1}{2}(1-2\nu_j) & 0 \\ 0 & 0 & 0 & 0 & 0 & \frac{1}{2}(1-2\nu_j) \end{bmatrix} . \tag{8}$$

The stationarity condition implies that Equation (6) must hold for any $\tilde{\mathbf{u}}_j(t)$. This leads to the final FE form of the equation of motion for a single finite element,

$$\mathbf{K}_j\, \mathbf{u}_j(t) \;+\; \mathbf{M}_j\, \frac{\partial^2}{\partial t^2}\mathbf{u}_j(t) \;=\; \mathbf{f}_j(t)\,. \tag{9}$$

$\mathbf{K}_j$ and $\mathbf{M}_j$ are the element stiffness matrix and the element mass matrix, respectively, and $\mathbf{f}_j(t)$ represents the nodal forces applied to element j. The definitions of $\mathbf{K}_j$, $\mathbf{M}_j$ and $\mathbf{f}_j(t)$ are readily determined by a comparison of Equations (6) and (12).

Assuming that the excitation and response is varying harmonically with the circular frequency ω, the equation of motion may in turn be written in terms of the complex amplitudes $\mathbf{U}_j(\omega)$ and $\mathbf{F}_j(\omega)$ of the displacement and the nodal forces,

$$\left(\mathbf{K}_j \;-\; \omega^2\mathbf{M}_j\right)\mathbf{U}_j(\omega) \;=\; \mathbf{F}_j(\omega)\,. \tag{10}$$

The stiffness and mass matrices are independent of the frequency and should therefore only be determined once and can then be used for solution at many frequencies. This is a computational advantage over the boundary element method where the matrices must be generated again at each frequency.

In real materials, a part of the vibration energy will be dissipated due to material damping. Usually the energy dissipation is frequency dependent, and it may furthermore depend on temperature and, in the case of soil, the degree of saturation. A good damping model is not easily implemented in the time domain. In particular hysteretic damping is not causal, *i.e.* the response at a material point is influenced by future excitation. On the other hand, any viscoelastic model will provide a causal response. The simplest possible viscoelastic model is linear viscous damping. This model is however not descriptive of most solid materials and soil, where the frequency dependence is not linear. Damping models based on the fractional time derivatives approach have been proven to be much more accurate and efficient than rational approximation models when a damping model is to be fitted in a broad frequency band.

In the frequency domain, material damping is implemented by introduction of the damping matrix $\mathbf{C}_j$, which enters the FE form of the equation of motion in the following way,

$$\left(\mathbf{K}_j + \gamma_j(\omega)\,\mathbf{C}_j - \omega^2\mathbf{M}_j\right)\mathbf{U}_j(\omega) = \mathbf{F}_j(\omega)\,. \tag{11}$$

Here the frequency dependence is represented by the function $\gamma_j(\omega)$. A hysteretic damping model implies that there is no frequency dependence, *i.e.* $\gamma_j(\omega) = i$. Usually, hysteretic damping is implemented in wave propagation problems by the introduction of a complex Young's modulus, $E_j^* = E_j(1 + i\eta_j)$, whereby the damping matrix for element j becomes $\mathbf{C}_j = \eta_j\mathbf{K}_j$. Here η_j is the *loss factor* for the material in element j. Any other material damping model is easily implemented by assuming the loss factor to be frequency dependent. Hence, the description of the energy dissipation in realistic materials is obtained by using a frequency dependent complex Young's modulus, $E_j^*(\omega) = E_j(1 + i\eta(\omega))$. It should be noted that at the present stage there is no possibility in BEASTS to enter a frequency dependent loss factor for the materials. To analyse models where a strong frequency dependence of the material damping is to be accounted for, BEASTS must be executed separately for each individual frequency.

The assembly of the local systems of equations is carried out by adding the contributions from all elements sharing the same degrees of freedom. This produces the system matrices $\mathbf{K}$, $\mathbf{C}$ and $\mathbf{M}$ for the entire domain, Ω. Thus, for a domain discretized with finite elements, the equation of motion reads

$$\left(\mathbf{K} + i\mathbf{C} - \omega^2\mathbf{M}\right)\mathbf{U}(\omega) = \mathbf{K}_{FE}(\omega)\,\mathbf{U}(\omega) = \mathbf{F}(\omega)\,. \tag{12}$$

where $\mathbf{K}_{FE}(\omega)$ is the complex, or dynamic, stiffness matrix. This dynamic stiffness matrix for the finite element part of a model and the point forces applied to the nodes of the finite elements may eventually be assembled into the global system of equations along with a number of boundary element domains as explained in Reference [3].

3 Three-dimensional Continuum Finite Elements

In the following subsections the shape functions for each of the finite element types available in BEASTS are given. All the finite elements described in this section are isoparametric continuum elements. While some of the elements have the same order of interpolation in all directions other elements have different orders of interpolation in different directions. Two element types are available: *hexahedral* (brick) elements and *triangular prismatic* (wedge) elements. In either case the shape functions are defined in a local, or 'homogeneous', (ξ_1, ξ_2, ξ_3)-coordinate system. A mapping into Cartesian space is carried out by means of the so-called *Jacobian*, the determinant of the matrix $\mathbf{J}$, which relates local derivatives to global derivatives,

$$dV = dx_1\,dx_2\,dx_3 = \det(\mathbf{J})\,d\xi_1\,d\xi_2\,d\xi_3, \quad \mathbf{J} = \begin{bmatrix} \frac{\partial x_1}{\partial \xi_1} & \frac{\partial x_1}{\partial \xi_2} & \frac{\partial x_1}{\partial \xi_3} \\ \frac{\partial x_2}{\partial \xi_1} & \frac{\partial x_2}{\partial \xi_2} & \frac{\partial x_2}{\partial \xi_3} \\ \frac{\partial x_3}{\partial \xi_1} & \frac{\partial x_3}{\partial \xi_2} & \frac{\partial x_3}{\partial \xi_3} \end{bmatrix}. \tag{13}$$

The subsections include figures that illustrate the node ordering used in BEASTS. An alternative node order, which resembles the node order used in ANSYS, may also be used. The order in which the nodes should appear in the input, when this ANSYS node order is used, is also indicated on the figures.

3.1 Hexahedron with 8 Nodes (Element Type 1)

The first class of elements is the so-called *hexahedral*, or brick, elements. For this class of elements, the local (ξ_1, ξ_2, ξ_3)-coordinate system has its origin at the centre of the element, which has the the dimensions $2 \times 2 \times 2$ in the homogeneous system. This applies to the elements described in this subsection and to the elements in Subsections 3.2 to 3.8.

The simplest possible hexahedral element that may be used for finite element analysis is the eight-noded element, which has linear interpolation of the geometry and the displacement field in all three local directions, ξ_1, ξ_2 and ξ_3. This kind of element may be particularly useful for the discretization of the thin, stiff parts in a model where relatively long wavelengths are expected compared to those in the remaining parts of the model. However, the linear elements are not well suited to a direct coupling with the boundary elements in BEASTS, where a biquadratic interpolation is used for the quadrilateral elements.

The node order used in BEASTS is illustrated on Figure 1a, and the corresponding shape functions are given in Equation (14). Figure 1b shows the alternative ANSYS node order.

$$\begin{aligned}
\phi_1 &= \tfrac{1}{8}(1-\xi_1)(1-\xi_2)(1-\xi_3), \quad \phi_2 = \tfrac{1}{8}(1+\xi_1)(1-\xi_2)(1-\xi_3), \\
\phi_3 &= \tfrac{1}{8}(1+\xi_1)(1+\xi_2)(1-\xi_3), \quad \phi_4 = \tfrac{1}{8}(1-\xi_1)(1+\xi_2)(1-\xi_3), \\
\phi_5 &= \tfrac{1}{8}(1-\xi_1)(1-\xi_2)(1+\xi_3), \quad \phi_6 = \tfrac{1}{8}(1+\xi_1)(1-\xi_2)(1+\xi_3), \\
\phi_7 &= \tfrac{1}{8}(1+\xi_1)(1+\xi_2)(1+\xi_3), \quad \phi_8 = \tfrac{1}{8}(1-\xi_1)(1+\xi_2)(1+\xi_3).
\end{aligned} \tag{14}$$

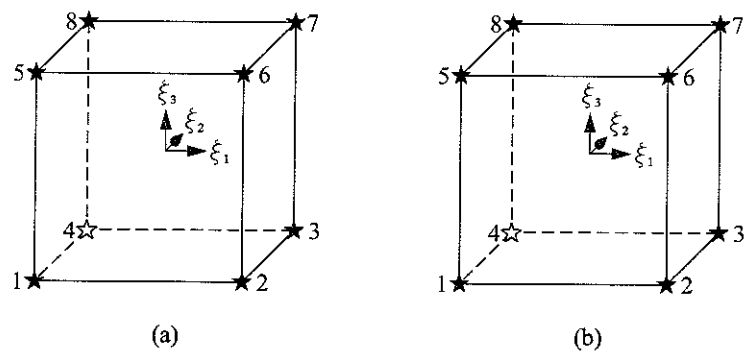

Figure 1. Hexahedral element with 8 nodes: (a) standard node order and (b) ANSYS node order.

3.2 Hexahedron with 18 Nodes (Element Type 2)

In order to obtain a conforming mesh, it is required that the shape functions for two adjacent elements be the same at the common interface. When, for example, thin tunnel walls or foundations are modelled, and quadratic interpolation is used for the boundary elements, a brick finite element with 18 nodes is advantageous. This element has quadratic interpolation in two of the local directions (here, the ξ_1 and ξ_2 directions) and linear interpolation in the third (the ξ_3) direction. Hence, for example, the total number of degrees of freedom for a tunnel wall would be the same as if the wall was modelled with nine-noded quadrilateral boundary elements. However, the boundary elements would not provide satisfactory results for a thin structure, unless an immense number of elements were used, as the distance between two surfaces/interfaces must be approximately one element length or more in the BEM due to the singularities of the Green's functions.

The node order used in BEASTS for the 18-noded hexahedral element is illustrated in Figure 2a, and the corresponding shape functions are given in Equation (15). Figure 2b shows the alternative ANSYS node order.

$$
\begin{aligned}
\phi_{\,1} &= \tfrac{1}{8}(\xi_1^2-\xi_1)(\xi_2^2-\xi_2)(1-\xi_3), & \phi_{\,2} &= \tfrac{1}{4}(1-\xi_1^2)(\xi_2^2-\xi_2)(1-\xi_3),\\
\phi_{\,3} &= \tfrac{1}{8}(\xi_1+\xi_1^2)(\xi_2^2-\xi_2)(1-\xi_3), & \phi_{\,4} &= \tfrac{1}{4}(\xi_1+\xi_1^2)(1-\xi_2^2)(1-\xi_3),\\
\phi_{\,5} &= \tfrac{1}{8}(\xi_1+\xi_1^2)(\xi_2+\xi_2^2)(1-\xi_3), & \phi_{\,6} &= \tfrac{1}{4}(1-\xi_1^2)(\xi_2+\xi_2^2)(1-\xi_3),\\
\phi_{\,7} &= \tfrac{1}{8}(\xi_1^2-\xi_1)(\xi_2+\xi_2^2)(1-\xi_3), & \phi_{\,8} &= \tfrac{1}{4}(\xi_1^2-\xi_1)(1-\xi_2^2)(1-\xi_3),\\
\phi_{\,9} &= \tfrac{1}{2}(1-\xi_1^2)(1-\xi_2^2)(1-\xi_3), & \phi_{10} &= \tfrac{1}{8}(\xi_1^2-\xi_1)(\xi_2^2-\xi_2)(1+\xi_3),\\
\phi_{11} &= \tfrac{1}{4}(1-\xi_1^2)(\xi_2^2-\xi_2)(1+\xi_3), & \phi_{12} &= \tfrac{1}{8}(\xi_1+\xi_1^2)(\xi_2^2-\xi_2)(1+\xi_3),\\
\phi_{13} &= \tfrac{1}{4}(\xi_1+\xi_1^2)(1-\xi_2^2)(1+\xi_3), & \phi_{14} &= \tfrac{1}{8}(\xi_1+\xi_1^2)(\xi_2+\xi_2^2)(1+\xi_3),\\
\phi_{15} &= \tfrac{1}{4}(1-\xi_1^2)(\xi_2+\xi_2^2)(1+\xi_3), & \phi_{16} &= \tfrac{1}{8}(\xi_1^2-\xi_1)(\xi_2+\xi_2^2)(1+\xi_3),\\
\phi_{17} &= \tfrac{1}{4}(\xi_1^2-\xi_1)(1-\xi_2^2)(1+\xi_3), & \phi_{18} &= \tfrac{1}{2}(1-\xi_1^2)(1-\xi_2^2)(1+\xi_3).
\end{aligned}
\tag{15}
$$

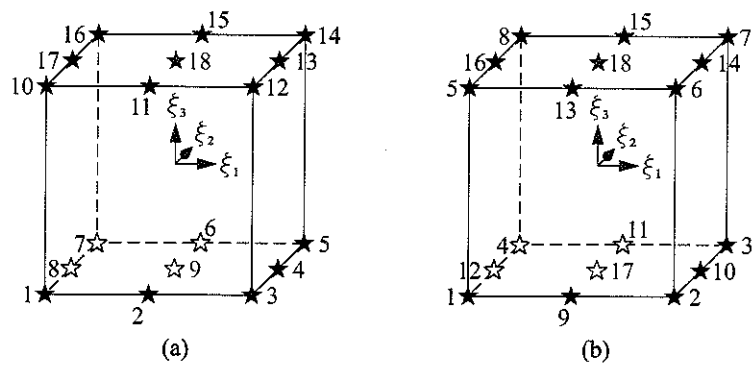

Figure 2. Hexahedral element with 18 nodes: (a) standard node order and (b) ANSYS node order.

3.3 Hexahedron with 26 Nodes (Element Type 3)

Continuum finite elements with quadratic interpolation in all directions may be suitable in parts of a model where the field quantities change rapidly with distance (*i.e.* the wavelengths are relatively short) and where inhomogeneities exist in one or more directions. In BEASTS a brick finite element with nine nodes on each side is provided. This element may be coupled to the quadrilateral boundary elements on any side. The node order for the 26-noded brick element is illustrated on Figure 3a with the corresponding shape functions given in Equation (16). Figure 3b shows the alternative ANSYS node order.

$$
\begin{aligned}
\phi_1 &= -\tfrac{1}{8}(\xi_1-\xi_1^2)(\xi_2-\xi_2^2)(\xi_3-\xi_3^2), & \phi_2 &= \tfrac{1}{4}(1-\xi_1^2)(\xi_2-\xi_2^2)(\xi_3-\xi_3^2),\\
\phi_3 &= \tfrac{1}{8}(\xi_1+\xi_1^2)(\xi_2-\xi_2^2)(\xi_3-\xi_3^2), & \phi_4 &= -\tfrac{1}{4}(\xi_1+\xi_1^2)(1-\xi_2^2)(\xi_3-\xi_3^2),\\
\phi_5 &= -\tfrac{1}{8}(\xi_1+\xi_1^2)(\xi_2+\xi_2^2)(\xi_3-\xi_3^2), & \phi_6 &= -\tfrac{1}{4}(1-\xi_1^2)(\xi_2+\xi_2^2)(\xi_3-\xi_3^2),\\
\phi_7 &= \tfrac{1}{8}(\xi_1-\xi_1^2)(\xi_2+\xi_2^2)(\xi_3-\xi_3^2), & \phi_8 &= \tfrac{1}{4}(\xi_1-\xi_1^2)(1-\xi_2^2)(\xi_3-\xi_3^2),\\
\phi_9 &= \tfrac{1}{6}(1-\xi_1^2)(1-\xi_2^2)(2\xi_3^2-3\xi_3+1), & \phi_{10} &= \tfrac{1}{4}(\xi_1-\xi_1^2)(\xi_2-\xi_2^2)(1-\xi_3^2),\\
\phi_{11} &= \tfrac{1}{6}(1-\xi_1^2)(2\xi_2^2-3\xi_2+1)(1-\xi_3^2), & \phi_{12} &= -\tfrac{1}{4}(\xi_1+\xi_1^2)(\xi_2-\xi_2^2)(1-\xi_3^2),\\
\phi_{13} &= \tfrac{1}{6}(2\xi_1^2+3\xi_1+1)(1-\xi_2^2)(1-\xi_3^2), & \phi_{14} &= \tfrac{1}{4}(\xi_1+\xi_1^2)(\xi_2+\xi_2^2)(1-\xi_3^2),\\
\phi_{15} &= \tfrac{1}{6}(1-\xi_1^2)(2\xi_2^2+3\xi_2+1)(1-\xi_3^2), & \phi_{16} &= -\tfrac{1}{4}(\xi_1-\xi_1^2)(\xi_2+\xi_2^2)(1-\xi_3^2),\\
\phi_{17} &= \tfrac{1}{6}(2\xi_1^2-3\xi_1+1)(1-\xi_2^2)(1-\xi_3^2), & \phi_{18} &= \tfrac{1}{8}(\xi_1-\xi_1^2)(\xi_2-\xi_2^2)(\xi_3+\xi_3^2),\\
\phi_{19} &= -\tfrac{1}{4}(1-\xi_1^2)(\xi_2-\xi_2^2)(\xi_3+\xi_3^2), & \phi_{20} &= -\tfrac{1}{8}(\xi_1+\xi_1^2)(\xi_2-\xi_2^2)(\xi_3+\xi_3^2),\\
\phi_{21} &= \tfrac{1}{4}(\xi_1+\xi_1^2)(1-\xi_2^2)(\xi_3+\xi_3^2), & \phi_{22} &= \tfrac{1}{8}(\xi_1+\xi_1^2)(\xi_2+\xi_2^2)(\xi_3+\xi_3^2),\\
\phi_{23} &= \tfrac{1}{4}(1-\xi_1^2)(\xi_2+\xi_2^2)(\xi_3+\xi_3^2), & \phi_{24} &= -\tfrac{1}{8}(\xi_1-\xi_1^2)(\xi_2+\xi_2^2)(\xi_3+\xi_3^2),\\
\phi_{25} &= -\tfrac{1}{4}(\xi_1-\xi_1^2)(1-\xi_2^2)(\xi_3+\xi_3^2), & \phi_{26} &= \tfrac{1}{6}(1-\xi_1^2)(1-\xi_2^2)(2\xi_3^2+3\xi_3+1).
\end{aligned}
\tag{16}
$$

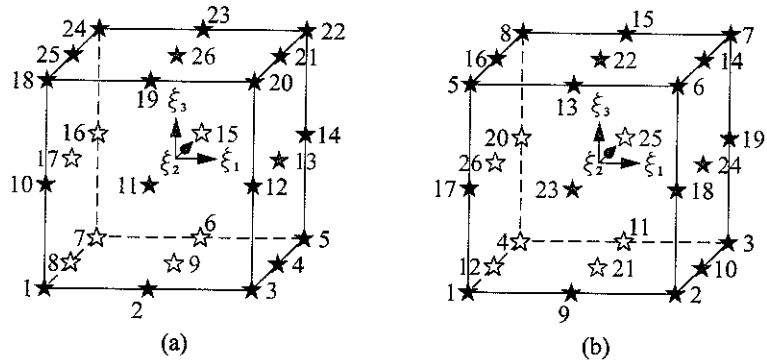

Figure 3. Hexahedral element with 26 nodes: (a) standard node order and (b) ANSYS node order.

3.4 Hexahedron with 21 Nodes (Element Type 4)

When finite elements of Type 2 are used to model a thin, infinite structure (*e.g.* a track) a situation may arise, where boundary element domains must be coupled with the finite element region as a means of providing radiating boundary conditions. In this case a transition element is necessary which has nine nodes on one side in addition to the two sides that already have nine nodes in Element Type 2. The node order used in BEASTS for a continuum element of this kind, that is an element with 21 nodes, is illustrated on Figure 4a. The corresponding shape functions are given in Equation (17), and on Figure 4b the alternative ANSYS node order is shown.

$$
\begin{aligned}
\phi_1 &= \tfrac{1}{8}(\xi_1^2-\xi_1)(\xi_2^2-\xi_2)(\xi_3^2-\xi_3), & \phi_2 &= \tfrac{1}{4}(1-\xi_1^2)(\xi_2^2-\xi_2)(\xi_3^2-\xi_3),\\
\phi_3 &= \tfrac{1}{8}(\xi_1+\xi_1^2)(\xi_2^2-\xi_2)(\xi_3^2-\xi_3), & \phi_4 &= \tfrac{1}{4}(\xi_1+\xi_1^2)(1-\xi_2^2)(1-\xi_3),\\
\phi_5 &= \tfrac{1}{8}(\xi_1+\xi_1^2)(\xi_2+\xi_2^2)(1-\xi_3), & \phi_6 &= \tfrac{1}{4}(1-\xi_1^2)(\xi_2+\xi_2^2)(1-\xi_3),\\
\phi_7 &= \tfrac{1}{8}(\xi_1^2-\xi_1)(\xi_2+\xi_2^2)(1-\xi_3), & \phi_8 &= \tfrac{1}{4}(\xi_1^2-\xi_1)(1-\xi_2^2)(1-\xi_3),\\
\phi_9 &= \tfrac{1}{2}(1-\xi_1^2)(1-\xi_2^2)(1-\xi_3), & \phi_{10} &= \tfrac{1}{4}(\xi_1^2-\xi_1)(\xi_2^2-\xi_2)(1-\xi_3^2),\\
\phi_{11} &= \tfrac{1}{2}(1-\xi_1^2)(\xi_2^2-\xi_2)(1-\xi_3^2), & \phi_{12} &= \tfrac{1}{4}(\xi_1^2+\xi_1)(\xi_2^2-\xi_2)(1-\xi_3^2),\\
\phi_{13} &= \tfrac{1}{8}(\xi_1^2-\xi_1)(\xi_2^2-\xi_2)(\xi_3^2+\xi_3), & \phi_{14} &= \tfrac{1}{4}(1-\xi_1^2)(\xi_2^2-\xi_2)(\xi_3^2+\xi_3),\\
\phi_{15} &= \tfrac{1}{8}(\xi_1+\xi_1^2)(\xi_2^2-\xi_2)(\xi_3^2+\xi_3), & \phi_{16} &= \tfrac{1}{4}(\xi_1+\xi_1^2)(1-\xi_2^2)(1+\xi_3),\\
\phi_{17} &= \tfrac{1}{8}(\xi_1+\xi_1^2)(\xi_2+\xi_2^2)(1+\xi_3), & \phi_{18} &= \tfrac{1}{4}(1-\xi_1^2)(\xi_2+\xi_2^2)(1+\xi_3),\\
\phi_{19} &= \tfrac{1}{8}(\xi_1^2-\xi_1)(\xi_2+\xi_2^2)(1+\xi_3), & \phi_{20} &= \tfrac{1}{4}(\xi_1^2-\xi_1)(1-\xi_2^2)(1+\xi_3),\\
\phi_{21} &= \tfrac{1}{2}(1-\xi_1^2)(1-\xi_2^2)(1+\xi_3).
\end{aligned}
\tag{17}
$$

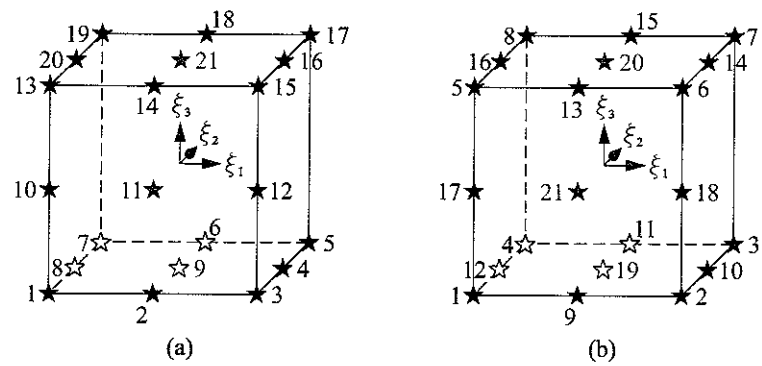

Figure 4. Hexahedral element with 21 nodes: (a) standard node order and (b) ANSYS node order.

3.5 Hexahedron with 13 Nodes (Element Type 5)

Transition elements are beneficial when finite elements with quadratic interpolation need to be used in parts of a model, but linear interpolation is sufficient in other parts of the model, where the wavelengths are much longer. In BEASTS a hexahedral element with 13 nodes is available. This element has 9 nodes and quadratic interpolation on one side, so that it may be coupled with finite elements of Type 2 or 3 or, alternatively, with the quadrilateral boundary elements. On the opposite side there are only four nodes, *i.e.* linear interpolation, whereby a conforming coupling to finite elements of Type 1 is possible.

The node order used in BEASTS for the 13-noded transition element is illustrated in Figure 5a with the corresponding shape functions given in Equation (18). Figure 5b shows the alternative ANSYS node order.

$$
\begin{aligned}
\phi_{\,1} &= \tfrac{1}{8}(\xi_1^2-\xi_1)(\xi_2^2-\xi_2)(1-\xi_3), & \phi_{\,2} &= \tfrac{1}{4}(1-\xi_1^2)(\xi_2^2-\xi_2)(1-\xi_3),\\
\phi_{\,3} &= \tfrac{1}{8}(\xi_1+\xi_1^2)(\xi_2^2-\xi_2)(1-\xi_3), & \phi_{\,4} &= \tfrac{1}{4}(\xi_1+\xi_1^2)(1-\xi_2^2)(1-\xi_3),\\
\phi_{\,5} &= \tfrac{1}{8}(\xi_1+\xi_1^2)(\xi_2+\xi_2^2)(1-\xi_3), & \phi_{\,6} &= \tfrac{1}{4}(1-\xi_1^2)(\xi_2+\xi_2^2)(1-\xi_3),\\
\phi_{\,7} &= \tfrac{1}{8}(\xi_1^2-\xi_1)(\xi_2+\xi_2^2)(1-\xi_3), & \phi_{\,8} &= \tfrac{1}{4}(\xi_1^2-\xi_1)(1-\xi_2^2)(1-\xi_3),\\
\phi_{\,9} &= \tfrac{1}{2}(1-\xi_1^2)(1-\xi_2^2)(1-\xi_3), & \phi_{10} &= \tfrac{1}{8}(\xi_1-1)(\xi_2-1)(\xi_3+1),\\
\phi_{11} &= \tfrac{1}{8}(1+\xi_1)(1-\xi_2)(1+\xi_3), & \phi_{12} &= \tfrac{1}{8}(1+\xi_1)(1+\xi_2)(1+\xi_3),\\
\phi_{13} &= \tfrac{1}{8}(1-\xi_1)(1+\xi_2)(1+\xi_3).
\end{aligned}
\tag{18}
$$

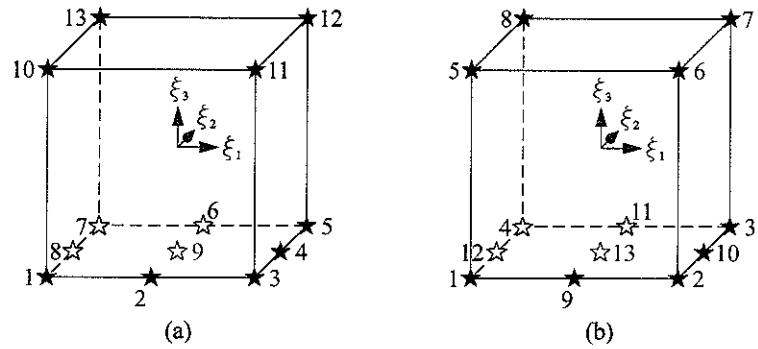

Figure 5. Hexahedral element with 13 nodes: (a) standard node order and (b) ANSYS node order.

3.6 Hexahedron with 17 Nodes (Element Type 6)

When elements of Type 5 are used to model a tunnel wall, a track or another thin structure of infinite extent, boundary element domains must be coupled with the finite elements at the artificial ends to ensure radiation of waves. Thus quadratic interpolation has to be used on two adjacent sides of the finite elements, not only on one of the sides. A 17-noded continuum element, which provides the transition from quadratic interpolation to linear interpolation in two directions, is available in BEASTS as Element Type 6. The node order used in BEASTS for the brick finite element with 17 nodes is illustrated on Figure 6a, and the corresponding shape functions are given in Equation (19). Figure 6b shows the alternative ANSYS node order.

$$
\begin{aligned}
\phi_1 &= \tfrac{1}{8}(\xi_1^2-\xi_1)(\xi_2-\xi_2^2)(\xi_3-\xi_3^2), & \phi_2 &= \tfrac{1}{4}(1-\xi_1^2)(\xi_2-\xi_2^2)(\xi_3-\xi_3^2),\\
\phi_3 &= \tfrac{1}{8}(\xi_1+\xi_1^2)(\xi_2-\xi_2^2)(\xi_3-\xi_3^2), & \phi_4 &= \tfrac{1}{16}(\xi_1+\xi_1^2)(1-\xi_2^2)(\xi_3^2-4\xi_3+3),\\
\phi_5 &= \tfrac{1}{8}(\xi_1+\xi_1^2)(\xi_2+\xi_2^2)(1-\xi_3), & \phi_6 &= \tfrac{1}{4}(1-\xi_1^2)(\xi_2+\xi_2^2)(1-\xi_3),\\
\phi_7 &= \tfrac{1}{8}(\xi_1^2-\xi_1)(\xi_2+\xi_2^2)(1-\xi_3), & \phi_8 &= \tfrac{1}{16}(\xi_1^2-\xi_1)(1-\xi_2^2)(\xi_3^2-4\xi_3+3),\\
\phi_9 &= \tfrac{1}{8}(1-\xi_1^2)(1-\xi_2^2)(\xi_3^2-4\xi_3+3), & \phi_{10} &= \tfrac{1}{16}(\xi_1^2-\xi_1)(\xi_2^2-4\xi_2+3)(1-\xi_3^2),\\
\phi_{11} &= \tfrac{1}{8}(1-\xi_1^2)(\xi_2^2-4\xi_2+3)(1-\xi_3^2), & \phi_{12} &= \tfrac{1}{16}(\xi_1^2+\xi_1)(\xi_2^2-4\xi_2+3)(1-\xi_3^2),\\
\phi_{13} &= \tfrac{1}{8}(\xi_1^2-\xi_1)(1-\xi_2)(\xi_3+\xi_3^2), & \phi_{14} &= \tfrac{1}{4}(1-\xi_1^2)(1-\xi_2)(\xi_3+\xi_3^2),\\
\phi_{15} &= \tfrac{1}{8}(\xi_1+\xi_1^2)(1-\xi_2)(\xi_3+\xi_3^2), & \phi_{16} &= \tfrac{1}{8}(1+\xi_1)(\xi_2+1)(\xi_3+1),\\
\phi_{17} &= \tfrac{1}{8}(1-\xi_1)(\xi_2+1)(\xi_3+1).
\end{aligned}
\tag{19}
$$

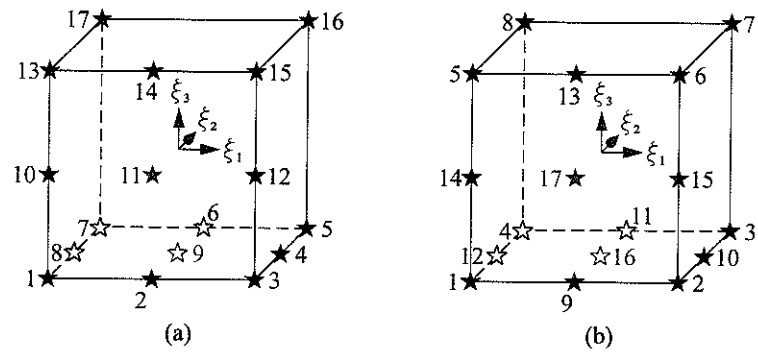

Figure 6. Hexahedral element with 17 nodes: (a) standard node order and (b) ANSYS node order.

3.7 Hexahedron with 20 Nodes (Element Type 7)

Finite elements with linear interpolation may be used to discretize the main part of a stiff structure of infinite or semi-infinite extent. However, to use the boundary elements available in BEASTS as a means of providing transmitting boundary conditions, a transition to elements with quadratic interpolation must be carried out. At the artificial corners an element is needed which has linear interpolation over three adjacent sides and quadratic interpolation over the three opposite sides. This 20-noded continuum element is available in BEASTS as Element Type 7. The node order used in BEASTS for the brick finite element with 20 nodes is illustrated on Figure 7a, and the corresponding shape functions are given in Equation (20). Figure 7b shows the alternative ANSYS node order.

$$
\begin{aligned}
\phi_1 &= \tfrac{1}{8}(\xi_1^2-\xi_1)(\xi_2^2-\xi_2)(\xi_3^2-\xi_3), & \phi_2 &= \tfrac{1}{4}(1-\xi_1^2)(\xi_2^2-\xi_2)(\xi_3^2-\xi_3),\\
\phi_3 &= \tfrac{1}{8}(\xi_1^2+\xi_1)(\xi_2^2-\xi_2)(\xi_3^2-\xi_3), & \phi_4 &= \tfrac{1}{4}(\xi_1^2+\xi_1)(1-\xi_2)(\xi_3^2-\xi_3),\\
\phi_5 &= \tfrac{1}{8}(\xi_1^2+\xi_1)(\xi_2^2+\xi_2)(\xi_3^2-\xi_3), & \phi_6 &= \tfrac{1}{16}(1-\xi_1^2)(\xi_2^2+\xi_2)(\xi_3^2-4\xi_3+3),\\
\phi_7 &= \tfrac{1}{8}(\xi_1^2-\xi_1)(\xi_2^2+\xi_2)(1-\xi_3), & \phi_8 &= \tfrac{1}{16}(\xi_1^2-\xi_1)(1-\xi_2^2)(\xi_3^2-4\xi_3+3),\\
\phi_9 &= \tfrac{1}{24}(1-\xi_1^2)(1-\xi_2^2)(5\xi_3^2-12\xi_3+7), & \phi_{10} &= \tfrac{1}{16}(\xi_1^2-\xi_1)(\xi_2^2-4\xi_2+3)(1-\xi_3^2),\\
\phi_{11} &= \tfrac{1}{24}(1-\xi_1^2)(5\xi_2^2-12\xi_2+7)(1-\xi_3^2), & \phi_{12} &= \tfrac{1}{4}(\xi_1^2+\xi_1)(\xi_2^2-\xi_2)(1-\xi_3^2),\\
\phi_{13} &= \tfrac{1}{24}(5\xi_1^2+12\xi_1+7)(1-\xi_2)(1-\xi_3^2), & \phi_{14} &= \tfrac{1}{16}(\xi_1^2+4\xi_1+3)(\xi_2^2+\xi_2)(1-\xi_3^2),\\
\phi_{15} &= \tfrac{1}{8}(\xi_1^2-\xi_1)(1-\xi_2)(\xi_3^2+\xi_3), & \phi_{16} &= \tfrac{1}{16}(1-\xi_1^2)(\xi_2^2-4\xi_2+3)(\xi_3^2+\xi_3),\\
\phi_{17} &= \tfrac{1}{8}(\xi_1^2+\xi_1)(\xi_2^2-\xi_2)(\xi_3^2+\xi_3), & \phi_{18} &= \tfrac{1}{16}(\xi_1^2+4\xi_1+3)(1-\xi_2^2)(\xi_3^2+\xi_3),\\
\phi_{19} &= \tfrac{1}{8}(1+\xi_1)(\xi_2^2+\xi_2)(\xi_3^2+\xi_3), & \phi_{20} &= \tfrac{1}{8}(1-\xi_1)(1+\xi_2)(1+\xi_3).
\end{aligned}
\tag{20}
$$

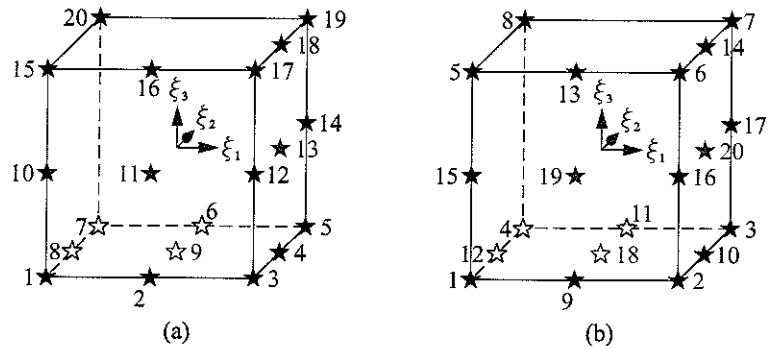

Figure 7. Hexahedral element with 20 nodes: (a) standard node order and (b) ANSYS node order.

3.8 Hexahedron with 23 Nodes (Element Type 8)

Elements of Type 2 may be used to model an embedded foundation or another thin structure, where a coupling is needed with a boundary element domain describing the surrounding soil. At the corners of such a structure, quadratic interpolation has to be used on two adjacent sides of the finite elements other than the sides, where quadratic interpolation is already used in elements of Type 2. A 23-noded continuum element, which may be used for this purpose, is available in BEASTS as Element Type 8. The node order used in BEASTS for the brick finite element with 23 nodes is illustrated on Figure 8a, and the corresponding shape functions are given in Equation (21). Figure 8b shows the alternative ANSYS node order.

$$
\begin{aligned}
\phi_1 &= \tfrac{1}{8}(\xi_1^2-\xi_1)(\xi_2^2-\xi_2)(\xi_3^2-\xi_3), & \phi_2 &= \tfrac{1}{4}(1-\xi_1^2)(\xi_2^2-\xi_2)(\xi_3^2-\xi_3),\\
\phi_3 &= \tfrac{1}{8}(\xi_1^2+\xi_1)(\xi_2^2-\xi_2)(\xi_3^2-\xi_3), & \phi_4 &= \tfrac{1}{4}(\xi_1^2+\xi_1)(1-\xi_2^2)(\xi_3^2-\xi_3),\\
\phi_5 &= \tfrac{1}{8}(\xi_1^2+\xi_1)(\xi_2^2+\xi_2)(\xi_3^2-\xi_3), & \phi_6 &= \tfrac{1}{4}(1-\xi_1^2)(\xi_2^2+\xi_2)(1-\xi_3),\\
\phi_7 &= \tfrac{1}{8}(\xi_1^2-\xi_1)(\xi_2^2+\xi_2)(1-\xi_3), & \phi_8 &= \tfrac{1}{4}(\xi_1^2-\xi_1)(1-\xi_2^2)(1-\xi_3),\\
\phi_9 &= \tfrac{1}{4}(1-\xi_1^2)(1-\xi_2^2)(\xi_3^2-2\xi_3+1), & \phi_{10} &= \tfrac{1}{4}(\xi_1^2-\xi_1)(\xi_2^2-\xi_2)(1-\xi_3^2),\\
\phi_{11} &= \tfrac{1}{4}(1-\xi_1^2)(\xi_2^2-2\xi_2+1)(1-\xi_3^2), & \phi_{12} &= \tfrac{1}{4}(\xi_1^2+\xi_1)(\xi_2^2-\xi_2)(1-\xi_3^2),\\
\phi_{13} &= \tfrac{1}{4}(\xi_1^2+2\xi_1+1)(1-\xi_2^2)(1-\xi_3^2), & \phi_{14} &= \tfrac{1}{4}(\xi_1^2+\xi_1)(\xi_2^2+\xi_2)(1-\xi_3^2),\\
\phi_{15} &= \tfrac{1}{8}(\xi_1^2-\xi_1)(\xi_2^2-\xi_2)(\xi_3^2+\xi_3), & \phi_{16} &= \tfrac{1}{4}(1-\xi_1^2)(\xi_2^2-\xi_2)(\xi_3^2+\xi_3),\\
\phi_{17} &= \tfrac{1}{8}(\xi_1^2+\xi_1)(\xi_2^2-\xi_2)(\xi_3^2+\xi_3), & \phi_{18} &= \tfrac{1}{4}(\xi_1^2+\xi_1)(1-\xi_2^2)(\xi_3^2+\xi_3),\\
\phi_{19} &= \tfrac{1}{8}(\xi_1^2+\xi_1)(\xi_2^2+\xi_2)(\xi_3^2+\xi_3), & \phi_{20} &= \tfrac{1}{4}(1-\xi_1^2)(\xi_2^2+\xi_2)(1+\xi_3),\\
\phi_{21} &= \tfrac{1}{8}(\xi_1^2-\xi_1)(\xi_2^2+\xi_2)(1+\xi_3), & \phi_{22} &= \tfrac{1}{4}(\xi_1^2-\xi_1)(1-\xi_2^2)(1+\xi_3),\\
\phi_{23} &= \tfrac{1}{4}(1-\xi_1^2)(1-\xi_2^2)(\xi_3^2+2\xi_3+1).
\end{aligned}
\tag{21}
$$

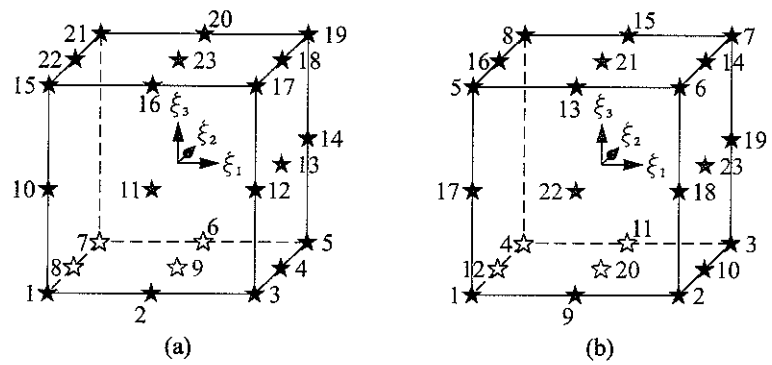

Figure 8. Hexahedral element with 23 nodes: (a) standard node order and (b) ANSYS node order.

3.9 Triangular Prism with 12 Nodes (Element Type 9)

In parts of a model where the mesh needs to refined, a transition from a coarser mesh may be carried out using *triangular prismatic*, or wedge, elements. A number of such finite elements are available in BEASTS. The local coordinate system for the wedge elements has its origin at one of the corners of the element, see Figure 9 for a definition of the coordinate directions. For convenience only, an extra coordinate $\xi^* = 1 - \xi_1 - \xi_2$ is introduced for use in the shape functions.

When elements of Type 2 are used to model a thin structure, wedge elements with quadratic interpolation in two directions and linear interpolation over the 'thickness' may be useful. The node order used in BEASTS for this wedge element with 12 nodes is illustrated on Figure 9a, and the corresponding shape functions are given in Equation (22). Figure 9b shows the alternative ANSYS node order.

$$
\begin{aligned}
\phi_1 &= \tfrac{1}{2}\xi_1(2\xi_1 - 1)(1 - \xi_3), \quad \phi_2 = 2\xi_1\xi_2(1 - \xi_3),\\
\phi_3 &= \tfrac{1}{2}\xi_2(2\xi_2 - 1)(1 - \xi_3), \quad \phi_4 = 2\xi_2\xi^*(1 - \xi_3),\\
\phi_5 &= \tfrac{1}{2}\xi^*(2\xi^* - 1)(1 - \xi_3), \quad \phi_6 = 2\xi^*\xi_1(1 - \xi_3),\\
\phi_7 &= \tfrac{1}{2}\xi_1(2\xi_1 - 1)(1 + \xi_3), \quad \phi_8 = 2\xi_1\xi_2(1 + \xi_3),\\
\phi_9 &= \tfrac{1}{2}\xi_2(2\xi_2 - 1)(1 + \xi_3), \quad \phi_{10} = 2\xi_2\xi^*(1 + \xi_3),\\
\phi_{11} &= \tfrac{1}{2}\xi^*(2\xi^* - 1)(1 + \xi_3), \quad \phi_{12} = 2\xi^*\xi_1(1 + \xi_3),
\end{aligned}
\tag{22}
$$

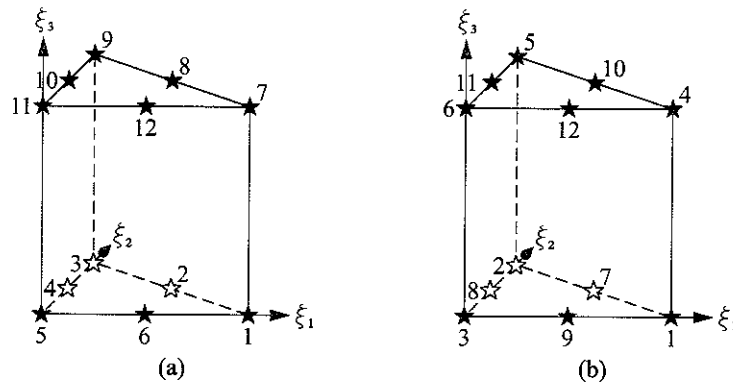

Figure 9. Wedge element with 12 nodes: (a) standard node order and (b) ANSYS node order.

3.10 Triangular Prism with 18 Nodes (Element Type 10)

In a structure where the thickness varies it may be necessary to use more elements over the thickness in some places than are necessary in other parts of the model. As transition elements between two such regions of a structure, for example, modelled with elements of Type 3, a wedge element with quadratic interpolation in all three directions is useful. The node order used in BEASTS for the wedge element with 18 nodes is illustrated on Figure 10a, and the corresponding shape functions are given in Equation (23) with $\xi^* = 1 - \xi_1 - \xi_2$. Figure 10b shows the alternative ANSYS node order.

$$
\begin{aligned}
\phi_1 &= \tfrac{1}{2}\xi_1(2\xi_1 - 1)(\xi_3^2 - \xi_3), & \phi_2 &= 2\xi_1\xi_2(\xi_3^2 - \xi_3),\\
\phi_3 &= \tfrac{1}{2}\xi_2(2\xi_2 - 1)(\xi_3^2 - \xi_3), & \phi_4 &= 2\xi_2\xi^*(\xi_3^2 - \xi_3),\\
\phi_5 &= \tfrac{1}{2}\xi^*(2\xi^* - 1)(\xi_3^2 - \xi_3), & \phi_6 &= 2\xi^*\xi_1(\xi_3^2 - \xi_3),\\
\phi_7 &= \xi_1(2\xi_1 - 1)(1 - \xi_3^2), & \phi_8 &= 4\xi_1\xi_2(1 - \xi_3^2),\\
\phi_9 &= \xi_2(2\xi_2 - 1)(1 - \xi_3^2), & \phi_{10} &= 4\xi_2\xi^*(1 - \xi_3^2),\\
\phi_{11} &= \xi^*(2\xi^* - 1)(1 - \xi_3^2), & \phi_{12} &= 4\xi^*\xi_1(1 - \xi_3^2),\\
\phi_{13} &= \tfrac{1}{2}\xi_1(2\xi_1 - 1)(\xi_3^2 + \xi_3), & \phi_{14} &= 2\xi_1\xi_2(\xi_3^2 + \xi_3),\\
\phi_{15} &= \tfrac{1}{2}\xi_2(2\xi_2 - 1)(\xi_3^2 + \xi_3), & \phi_{16} &= 2\xi_2\xi^*(\xi_3^2 + \xi_3),\\
\phi_{17} &= \tfrac{1}{2}\xi^*(2\xi^* - 1)(\xi_3^2 + \xi_3), & \phi_{18} &= 2\xi^*\xi_1(\xi_3^2 + \xi_3),
\end{aligned}
\tag{23}
$$

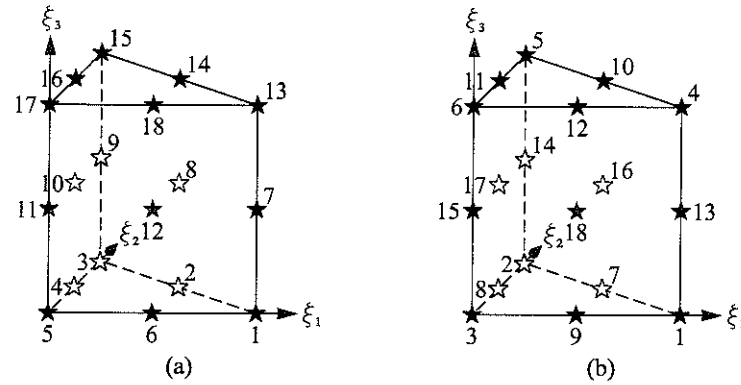

Figure 10. Wedge element with 18 nodes: (a) standard node order and (b) ANSYS node order.

3.11 Triangular Prism with 15 Nodes (Element Type 11)

A wedge element with quadratic interpolation on the two triangular surfaces and on one of the quadrilateral surfaces is provided in BEASTS as element Type 11. This 15 noded wedge element may be used in conjunction with elements of Type 4 in the transition between parts of a structure modelled with elements of Type 2 and 3, respectively. Furthermore, this kind of element is particularly useful when a coupling must be established with a BE sub-domain providing the artificial boundary conditions for a thin structure of infinite extent. The node order used in BEASTS for the wedge element with 15 nodes is illustrated on Figure 11a, and the corresponding shape functions are given in Equation (24) with $\xi^* = 1 - \xi_1 - \xi_2$. Figure 11b shows the alternative ANSYS node order.

$$
\begin{aligned}
&\phi_1 = \tfrac{1}{2}\xi_1(2\xi_1 - 1)(\xi_3^2 - \xi_3), && \phi_2 = 2\xi_1\xi_2(\xi_3^2 - \xi_3),\\
&\phi_3 = \tfrac{1}{2}\xi_2(2\xi_2 - 1)(\xi_3^2 - \xi_3), && \phi_4 = 2\xi_2\xi^*(1 - \xi_3),\\
&\phi_5 = \tfrac{1}{2}\xi^*(2\xi^* - 1)(1 - \xi_3), && \phi_6 = 2\xi^*\xi_1(1 - \xi_3),\\
&\phi_7 = \xi_1(2\xi_1 - 1)(1 - \xi_3^2), && \phi_8 = 4\xi_1\xi_2(1 - \xi_3^2),\\
&\phi_9 = \xi_2(2\xi_2 - 1)(1 - \xi_3^2), && \phi_{10} = \tfrac{1}{2}\xi_1(2\xi_1 - 1)(\xi_3^2 + \xi_3),\\
&\phi_{11} = 2\xi_1\xi_2(\xi_3^2 + \xi_3), && \phi_{12} = \tfrac{1}{2}\xi_2(2\xi_2 - 1)(\xi_3^2 + \xi_3),\\
&\phi_{13} = 2\xi_2\xi^*(1 + \xi_3), && \phi_{14} = \tfrac{1}{2}\xi^*(2\xi^* - 1)(1 + \xi_3),\\
&\phi_{15} = 2\xi^*\xi_1(1 + \xi_3),
\end{aligned}
\tag{24}
$$

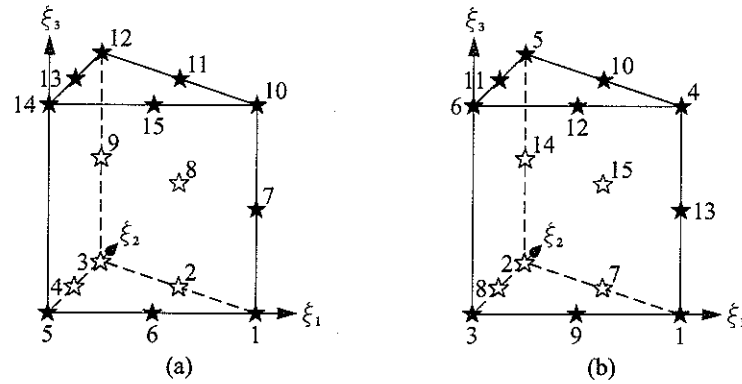

Figure 11. Wedge element with 15 nodes: (a) standard node order and (b) ANSYS node order.

4 Data Preparation

This section describes how the input data for a finite element domain should be organised in the global input data file for a BEASTS project.

4.1 General Data Specification

In addition to the modules mentioned in TM 868, the following module is now available:

**finite elements*

4.2 The **Finite Elements* Module

Syntax: The **finite elements* module has the following syntax:

```
*finite elements
   type   mat.no.   node1   node2   ...   nodeN
   type   mat.no.   node1   node2   ...   nodeN
    ⋮       ⋮        ⋮       ⋮              ⋮
   type   mat.no.   node1   node2   ...   nodeN
```

Description: This module is optional and may appear only once (*i.e.* all finite elements are defined in *one* domain). The number of finite elements that may be used is controlled by a parameter in the maximum dimensions file.

A single line of input data in the **finite elements* module defines the element type (data item 1), the material (data item 2) and the element topology (the remaining items of data) of one finite element. Currently there are 11 element types available in BEASTS. They are three-dimensional viscoelastic continuum elements with different order of interpolation and, as a result of this, with varying number of nodes. All materials used in the **finite elements* module must be defined in the **material properties* module.

The topology for the elements should contain the global node numbers corresponding to each of the `N` nodes in the element, where `N` is determined by the element type. Hence, a single line of data will contain $\mathtt{N}+2$ integers. The six finite element types available in BEASTS are all continuum elements. The number of nodes and the order of interpolation in each type of element are listed in Table 1. The order in which node numbers should be given depends on whether the standard node order or the ANSYS node order is used. Figures 1 to 9 show the node order in the two cases along with the geometry of the elements.

The *+Copy Elements* Option

Syntax: The *+copy elements* option has the following syntax:

```
+copy elements
   elem1   elem2   nodestep   NoC
```

The `NoC` (number of copies) parameter is optional. `NoC` is set to 1 if no other value is given.

Table 1. Finite element types in BEASTS. The order of interpolation and the number of Gauss points are listed for the ξ_1, the ξ_2 and the ξ_3 directions. Node orders are given in Figures 1 to 11.

Type	Shape	Nodes	Order of Interpolation	Gauss Points
1	Brick	8	Linear, linear, linear	2×2×2
2	Brick	16	Quadratic, quadratic, linear	3×3×2
3	Brick	26	Quadratic, quadratic, quadratic	3×3×3
4	Brick	21	Quadratic, quadratic, quadratic/linear	3×3×3
5	Brick	13	Quadratic/linear, quadratic/linear, linear	3×3×2
6	Brick	17	Quadratic/linear, quadratic/linear, quadratic/linear	3×3×3
7	Brick	20	Quadratic/linear, quadratic/linear, quadratic/linear	3×3×3
8	Brick	23	Quadratic, quadratic, quadratic/linear	3×3×3
9	Wedge	12	Quadratic, quadratic, linear	3×3×2
10	Wedge	18	Quadratic, quadratic, quadratic	3×3×3
11	Wedge	15	Quadratic, quadratic, quadratic/linear	3×3×3

Description: Instead of giving the topology for all elements in the FE region, a few of the elements may be defined in the standard way and the rest of them may be generated using the *+copy elements* option. This option is identical to the *+copy elements* option for boundary elements which is available within the **boundary element domain* module.

The *+copy elements* option has four items of data. The parameters `elem1` and `elem2` define an array of elements that should be copied. `elem1` must be less than `elem2` or, alternatively, equal to `elem2` in which case only one element is copied. The parameter `nodestep` defines the increment in node numbers between the original elements' topology and the new elements' topology. Finally `NoC` defines the number of copies that should be taken of the original elements. The node numbers will be further increased by `nodestep` in each successive copy.

The *+Move Elements* Option

Syntax: The *+move elements* option has the following syntax:

```
+move elements
   elem1   elem2   nodestep
```

Description: It may sometimes be necessary to move a part of the model which has been discretized with the use of finite elements to another position. This is, for example, the case when a longer tunnel section has to be analysed than first expected and the finite elements at the end of the tunnel are of another kind than those in the remaining part of the structure. Using the standard method of input, the entire set of data defining the element topology for those finite elements would have to be changed. However, a number of elements may be moved at once with the *+move elements* option.

The *+move elements* option has three items of data. The parameters `elem1` and `elem2` define an array of elements that should be moved. `elem1` must be less than `elem2` or, alternatively, equal to `elem2` in which case only one element is copied. The parameter `nodestep` defines

the increment in node numbers between the original elements' topology and the new elements' topology. In contrast to the *+copy elements* option, the original elements are eliminated .

The *+ANSYS Node Order* Option

Syntax: The *+ANSYS node order* option has the following syntax:

```
+ANSYS node order
```

Description: This option shifts the local interpretation of the element topology into ANSYS mode for the rest of the **finite elements* module. However, any succeeding **boundary element domain* modules will still use the global topology interpretation mode set by either the **ANSYS node order* module or the **standard node order* module.

The *+Standard Node Order* Option

Syntax: The *+standard node order* option has the following syntax:

```
+standard node order
```

Description: Similar to the *+ANSYS node order* option, this is a local version of the **standard node order* module.

4.3 The **Boundary Element Domain* Module, revisited

In addition to the options listed for the **boundary element domain* module in TM 868, the *+move elements* option explained above in the description of the **finite elements* module is also available in the **boundary element domain* module. The input data of the boundary element version is identical to that of the finite element version. Therefore, no further explanation is needed.

4.4 Setting the Number of Nodes Allowed in the Input Data

As a new feature, the number of nodes allowed in the global input file read by FLIES may be set independently of the number of nodes allowed in the final scheme used for analysis in ANTS. However, the maximum number of nodes allowed in the input data file should always be higher than the number of nodes allowed in the analysis. The maximum number of nodes allowed in the input is set by the parameter `nemax` in the include file `maxdim.inc`. The maximum number of nodes allowed in the analysis is still set by the parameter `nnmax`, see TM 868.

It may be advantageous to define more nodes than actually needed in a given model. For example, it makes the definition of finite elements much easier if all nodes in one layer of nodes are copied into the next layer, even if most of the nodes are going to be redundant. If the nodes have been defined for a wider space than is used in a model, it is a straight forward process to add new elements outside the existing ones, should this be necessary. Furthermore, with the new *+move elements* option available in both the **boundary element domain* and the **finite elements* modules, elements are easily moved to other parts of the model, if the nodes have been defined beforehand.

5 Numerical Examples

In this section a numerical example is given where a square foundation resting on a layered half-space is subject to either a vertical or a horizontal point load. Comparisons are made between a model where the foundation is discretized with finite elements, and two models, where boundary elements are used to discretize the foundation. The models are also used to investigate whether the horizontal excitation of the foundation will lead to a primarily translational or a primarily rotational movement of the foundation.

5.1 Case 1: Vertically Excited Foundation on a Layered Half-Space

A square concrete foundation with a side length of 4 metres and a depth of 0.5 metres is considered. The foundation rests on a 2 metre thick layer of soft clay, which lies on top of a half-space consisting of a stiffer clay. The properties for the three materials are given in Table 2, where E is the Young's modulus, ν is the Poisson ratio, ρ is the mass density, and η is the loss factor. Hysteretic damping is assumed.

Table 2. Parameters for layered half-space and concrete foundation.

Layer	E [MPa]	ν	ρ [kg/m^3]	η	Depth [m]
Foundation	20,000	0.15	2500	0.03	0.5
1 (Soft clay)	60	0.44	1500	0.10	2.0
2 (Stiff clay)	360	0.49	2000	0.10	∞

A vertical, harmonically varying, point force is applied at the centre of the foundation, and the response is analysed at the three frequencies 10, 20 and 30 Hz. Three models are used for comparison (see BEASTS input data files in Appendices A and B):

1. The foundation is modelled with finite elements of Type 2, see Subsection 3.2. Each element has the dimensions $2 \times 2 \times 0.5$ m^3. The layer and the half-space underneath are both modelled using quadrilateral boundary elements with the dimensions 2×2 m^2.

2. Boundary elements are used in all parts of the model. The dimensions of the boundary elements used for the foundation correspond to those of the finite elements used in the first model.

3. As in Model 2, the discretization is carried out entirely by the use of boundary elements. However, the mesh is refined so that the distance between the top and the bottom of the foundation corresponds to the length of one element.

In all models the plane of symmetry in one of the directions has been utilized to reduce the number of degrees of freedom and hence the computation time. The combined FE/BE mesh used for the discretization in Model 1 is visualized in Figure 12, and the refined boundary element mesh used in Model 3 is shown in Figure 13. The mesh in Model 2 is similar to that in Model 1, except that boundary elements are used instead of the finite elements for the foundation, *i.e.* the green lines should be replaced with blue lines.

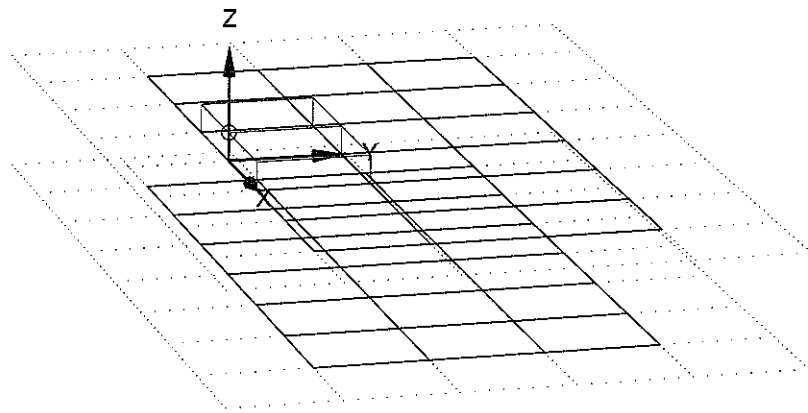

Figure 12. Mesh used for the discretization in Model 1. Green lines indicate finite elements, whereas blue lines indicate boundary elements. Elements drawn with dotted lines are only used for calculation of the singular diagonal terms of the traction Green's function matrix, see Reference [3].

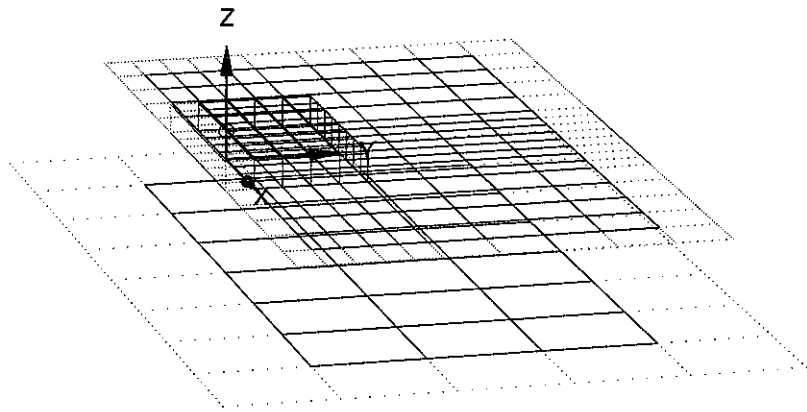

Figure 13. The refined mesh used for the discretization in Model 3.

Figure 14 shows the wave propagation pattern obtained in each analysis. The foundation is not shown in the figure. However, the edge of the foundation is readily seen, in particular for Models 1 and 3 at the frequency 20 Hz. Here the wave fronts on the surface of the ground are almost quadratic when they leave the foundation, but farther away from the point of excitation they become circular.

The results achieved in Models 1 and 3 are very similar. The fact that the finite element model provides good results is further demonstrated in Table 3. Here the difference in the vertical displacement amplitude response for Models 2 and 3 are given relative to the response in Model 1 for the point on the surface of the ground located directly under the point of excitation. The difference between the results obtained in Models 1 and 3 is 10-15%, slightly higher at 10 Hz than at 30 Hz.

Model 2, on the other hand, provides results which are significantly different from the results gained with the other two models. At the surface of the ground directly under the point of excitation, a difference of more than 30% is obtained at 10 Hz compared with the results of Model 1. For higher frequencies the difference is even greater, see Table 3.

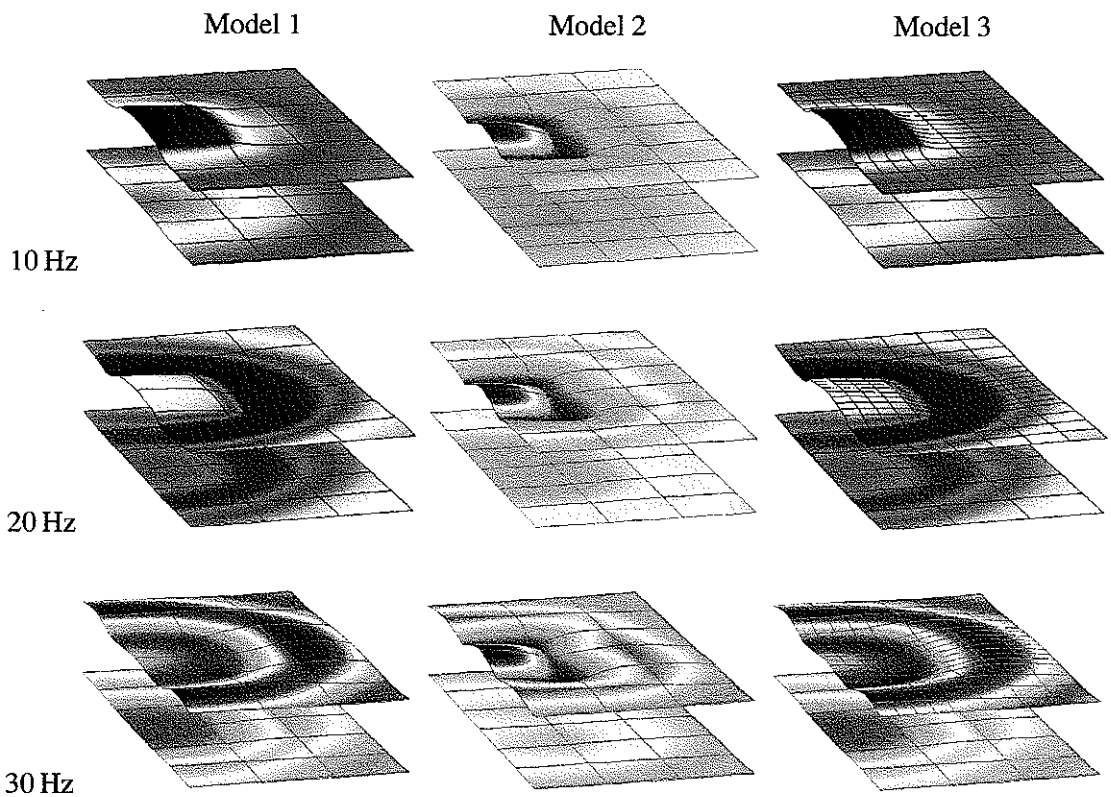

Figure 14. Instantaneous displacements of the surface of the ground and of the interface between the top-layer and the half-space for a vertically excited foundation. Green colour indicates small vertical displacements, whereas blue and red colours indicate negative and positive vertical displacements, respectively. The scale used for displacements as well as the colour scale are identical in the three models and for the three frequencies.

Table 3. Difference in the vertical displacement amplitude response at the point on ground surface directly under the excitation point.

Difference	10 Hz	20 Hz	30 Hz
Models 1 & 2	0.3383	0.5678	0.8773
Models 1 & 3	0.1454	0.1276	0.0978

Table 4. Horizontal displacement amplitudes at the ground surface under the centre of the foundation.

Model	10 Hz	20 Hz	30 Hz
1	$2.22 \cdot 10^{-14}$	$7.64 \cdot 10^{-15}$	$9.87 \cdot 10^{-15}$
2	$3.01 \cdot 10^{-10}$	$1.18 \cdot 10^{-10}$	$6.19 \cdot 10^{-11}$
3	$1.29 \cdot 10^{-12}$	$1.25 \cdot 10^{-12}$	$4.82 \cdot 10^{-13}$

It is clear, that the difference in the response is due to erroneous results from the analysis with the model, in which only a few boundary elements are used in the discretization of the foundation, *i.e.* Model 2. Not only are the wave fronts not circular at a certain distance, as it would be expected, but the displacement response is not symmetric with respect to the *second* plane of symmetry in the model, *i.e.* the one that has not been used to reduce the number of degrees of freedom.

Table 4 lists the horizontal displacement amplitudes at the point on the ground surface under the centre of the foundation (for comparison, it must be noted that the vertical displacement amplitude is of the order 10^{-9} for all frequencies at this point). Here, the horizontal displacement is supposed to be zero because of the symmetry, but, due to numerical errors in the integration scheme, small discrepancies would be expected. This is the case for Models 1 and 3 (it is noticed that the errors in Model 1 are in fact smaller than those in Model 3), whereas in Model 2, the error is quite significant. Thus the horizontal displacement amplitude is only one order of magnitude smaller than the vertical displacement amplitude.

Thus, a thin, stiff foundation on top of a layered half-space may be analysed by either finite elements combined with boundary elements or with boundary elements alone. However, to obtain results with satisfactory accuracy, the number of degrees of freedom that must be used in the pure BE model is much higher than that in the combined model. Hence, for the present kind of structure, a combined FE/BE scheme is much more efficient. In the present analysis the computation time per frequency on a PIII 450 MHz PC was 3 and 4 minutes for Models 1 and 2, respectively, whereas 2 hours and 32 minutes were required for the analysis with Model 3. A reduction of the computation time for Model 3 could be achieved by using fewer elements on the part of the surface of the ground which is not in contact with the foundation. A further refinement with the use of triangular elements would be needed for this purpose. However, the computation time for a refined BE model would still be much longer than the computation time for the FE/BE model.

5.2 Case 2: Horizontally Excited Foundation on a Layered Half-Space

Next, the response of the square foundation on the layered half-space due to horizontal excitation is investigated. For comparison, the analysis is carried out with the same three models that were used for the analysis in Subsection 5.1. In Figure 15 the wave propagation pattern is illustrated at the three frequencies 10, 20 and 30 Hz, and for an arbitrary phase angle.

Looking at Figure 15 it may again be concluded that the results obtained with Models 1 and 3 are similar and very different from the results produced with Model 2. In particular the response at the corners of the foundation seems to be overestimated in the analysis with Model 2. Furthermore, in Model 2 the foundation is undergoing strong deformations, even at the low frequency of 10 Hz. Here a concrete foundation with the given dimensions would be expected to behave almost like a stiff body - the behaviour which can be observed in Models 1 and 3. In the case of horizontal excitation, a purely anti-symmetric response is expected. Whereas Models 1 and 3 produce results which fulfill this criteria, the response achieved with Model 2 is not perfectly anti-symmetric.

The response is studied at the point which lies on the X-axis at the edge of the foundation, *i.e.* at coordinates (-2,0,0), see Figure 12. The ratios $|U_1|/|U_3|$ between the absolute values of the horizontal displacement amplitude and the vertical displacement amplitude at this point are

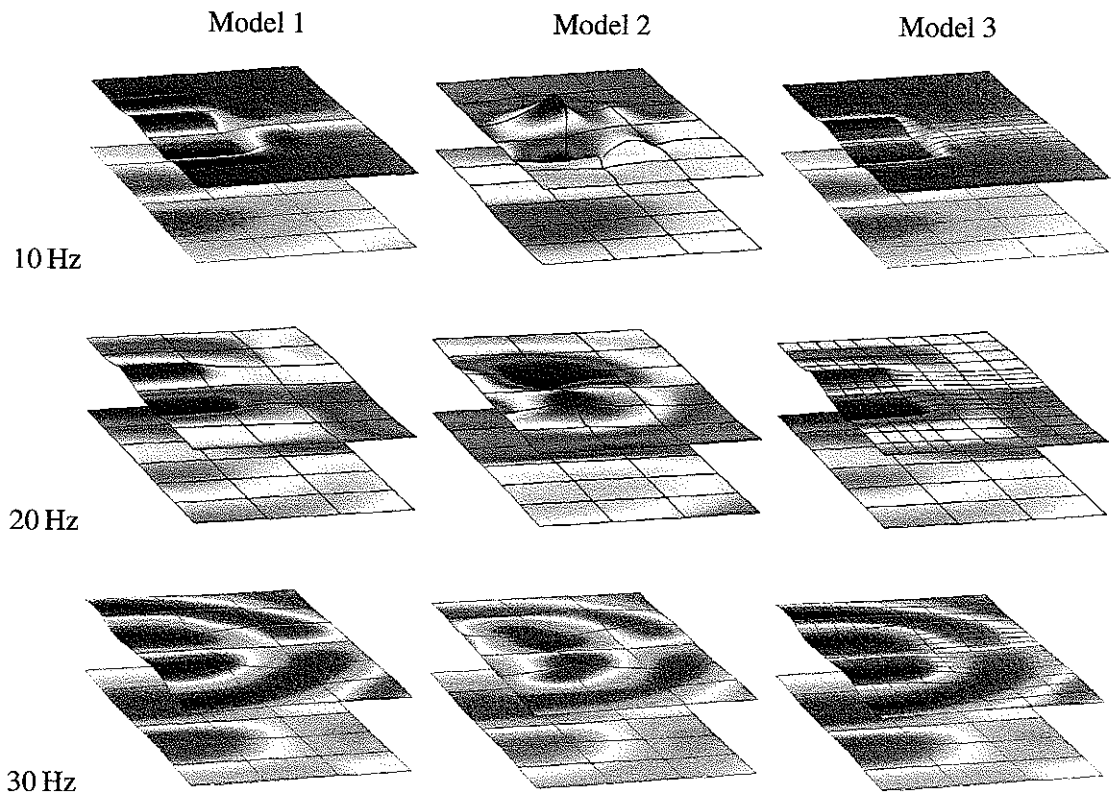

Figure 15. Instantaneous displacements of the surface of the ground and of the interface between the top-layer and the half-space for a horizontally excited foundation. Green colour indicates small vertical displacements, whereas blue and red colours indicate negative and positive vertical displacements, respectively. The scale used for displacements as well as the colour scale are identical in the three models and for the three frequencies.

Table 5. Ratio between horizontal and vertical displacement amplitude at the edge of the foundation.

Model	10 Hz	20 Hz	30 Hz
1	9.512	1.7115	1.6722
2	13.592	12.595	3.8909
3	8.5088	1.6548	1.7637

given in Table 5. A big ratio indicates that the translation part of the motion is dominating, whereas a small ratio indicates that the rotation is dominating. A vertical translation of the foundation is not possible because the response is anti-symmetric.

From the values listed in Table 5, it is observed that the motion is almost a pure translation at the frequency 10 Hz (Models 1 and 2). For the higher frequencies, there is a much stronger rotation, though the translation is still dominating. Model 2 overestimates the translation (or underestimates the rotation), and the results gained with this model are generally poor.

6 Conclusions

A number of different three-dimensional continuum finite elements have been implemented in the boundary element analysis program BEASTS. Hence, BEASTS may now be used for coupled finite element/boundary element analysis of elastodynamic three-dimensional problems in the frequency domain. The finite elements may be used to model parts of a structure, where local inhomogeneities exist, or where boundary elements are inconvenient because the structure is stiff and thin.

As a test of the implemented elements, a thin, stiff foundation resting on a layered half-space has been analysed. A coupled FE/BE scheme where finite elements are used to model the foundation and boundary elements are used to discretize the surrounding soil, has been found to be much more efficient than a model, in which only boundary elements are used. In these circumstances, it can be concluded that boundary elements need to be much smaller than finite elements to provide satisfactory results.

Acknowledgement

L. Andersen would like to thank the Danish Technical Research Council for financial support via the research project: 'Damping Mechanisms in Dynamics of Structures and Materials'.

References

[1] J. D. Achenbach. *Wave Propagation in Elastic Solids*. North-Holland Publishing Company, Amsterdam, 1 edition, 1973.

[2] L. Andersen and C.J.C. Jones. BEASTS - A Computer Program for Boundary Element Analysis of Soil and Three-dimensional Structures. ISVR Technical Memorandum 868, Institute of Sound and Vibration Research, University of Southampton, Southampton SO17 1BJ, England, October 2001.

[3] L. Andersen and C.J.C. Jones. Three-Dimensional Elastodynamic Analysis Using Multiple Boundary Element Domains. ISVR Technical Memorandum 867, Institute of Sound and Vibration Research, University of Southampton, Southampton SO17 1BJ, England, October 2001.

A BEASTS input: Model 1

This is the input file for the computer program BEASTS used for the coupled finite element and boundary element analysis (Model 1) of a quadratic foundation on a layered half-space in Section 5. In the present case a vertical point force is applied at the centre of the foundation.

```
*title

 Foundation on layered half-space - LA 31/10/2001

*material

   60E6  0.44  1500.0  0.1000 ! Soft clay (top layer)
  360E6  0.49  2000.0  0.1000 ! Stiff clay (half-space)
  200E8  0.15  2500.0  0.0300 ! Concrete (foundation)

*frequency

  10.0
  20.0
  30.0

*multi file output

*plane of symmetry

*node coordinates

 -8.0 0.0 0.0

 +offset
  1 1 1.0 0.0 0.0 16

 +offset
  1 17 0.0 1.0 0.0 8

 +offset
  1 153 0.0 0.0 -2.0

 +offset
  1 153 0.0 0.0 0.50 2

*boundary element domain 1 - the top layer

  1 ! Use material 1 - soft clay

  1 2 3 20 37 36 35 18 19

 +copy
  1 1 2 7
```

```
 +copy
  1 8 34 3

 +mirror copy
  1 32 153

*boundary element domain 2 - the half-space

  2 ! Use material 2 - stiff clay

  154 155 156 173 190 189 188 171 172

 +copy
  1 1 2 7

 +copy
  1 8 34 3

*finite elements - the foundation

  2 3 7 8 9 26 43 42 41 24 25 313 314 315 332 349 348 347 330 331

 +copy
  1 1 2

*loads

  315 0.0 0.0 0.0 0.0 1.0 0.0 ! Vertical point load on foundation

*end
```

B BEASTS input: Model 2

This is the input file for the computer program BEASTS used for the boundary element analysis (Model 3) of a quadratic foundation on a layered half-space in Section 5. In the present case a vertical point force is applied at the centre of the foundation.

```
*title

 Foundation on layered half-space - LA 31/10/2001

*material

   60E6  0.44  1500.0  0.1000 ! Soft clay (top layer)
  360E6  0.49  2000.0  0.1000 ! Stiff clay (half-space)
  200E8  0.15  2500.0  0.0300 ! Concrete (foundation)

*frequency

  10.0
  20.0
  30.0

*multi file output

*plane of symmetry

*node coordinates

 -8.0 0.0 -2.0

 +offset
  1 1 1.0 0.0 0.0 16

 +offset
  1 17 0.0 1.0 0.0 8

 -7.0 0.0 0.0

 +offset
  154 154 0.25 0.0 0.0 56

 +offset
  174 190 0.0 0.0 0.25 2

 +offset
  236 236 0.0 0.0 0.25 9

 +offset
  154 253 0.0 0.25 0.0 28
```

```
*boundary element domain 1 - the top layer

  1 ! Use material 1 - soft clay

  154 156 158 258 358 356 354 254 256
  174 175 176 276 376 375 374 274 275
  190 192 194 294 394 392 390 290 292

 +copy
  1 1 4 4

 +copy
  2 2 2 7

 +copy
  3 3 4 4

 +copy
  1 18 200 3

 954 956 958 1158 1358 1356 1354 1154 1156
 974 975 976 1176 1376 1375 1374 1174 1175
 990 992 994 1194 1394 1392 1390 1190 1192

 +copy
  73 73 4 4

 +copy
  74 74 2 7

 +copy
  75 75 4 4

 +copy
  73 90 400 4

 3 2 1 18 35 36 37 20 19

 +copy
  163 163 2 7

 +copy
  163 170 34 3

*boundary element domain 2 - the half-space

  2 ! Use material 2 - stiff clay

 +mirror on

  3 2 1 18 35 36 37 20 19
```

```
 +copy
  1 1 2 7

 +copy
  1 8 34 3

*boundary element domain 3 - the foundation

  3 ! use material 3 - concrete

  176 175 174 274 374 375 376 276 275

 +copy
  1 1 2 7

 +copy
  1 8 200 3

 +mirror copy
  1 32 54

  374 274 174 211 228 328 428 411 311

 +copy
  65 65 200 3

 +mirror copy
  65 68 16

  976 975 974 1011 1028 1029 1030 1013 1012

 +copy
  73 73 2 7

*loads

  236 0.0 0.0 0.0 0.0 1.0 0.0 ! Vertical point load on foundation

*end
```